European Journal of Pharmaceutics and Biopharmaceutics 71 (2009) 387–394

Contents lists available at ScienceDirect

European Journal of Pharmaceutics and Biopharmaceutics

journal homepage: www.elsevier.com/locate/ejpb

Research paper

Mechanism of drug release from polymethacrylate-based extrudates and milled strands prepared by hot-melt extrusion

Jessica Albers [a], Rainer Alles [b], Karin Matthée [a], Klaus Knop [a], Julia Schulze Nahrup [b], Peter Kleinebudde [a,*]

[a] Institute of Pharmaceutics and Biopharmaceutics, Heinrich-Heine-University, Duesseldorf, Germany
[b] Gen-Plus GmbH & Co. KG, Munich, Germany

ARTICLE INFO

Article history:
Received 20 June 2008
Accepted in revised form 6 October 2008
Available online 11 October 2008

Keywords:
Celecoxib
Polymethacrylate
Hot-melt extrusion
Solid dispersion
Dissolution
Intrinsic dissolution
Stability
Recrystallization inhibition

ABSTRACT

The aim of the study was the formulation of solid dispersions of the poorly water-soluble drug celecoxib and a polymethacrylate carrier by hot-melt extrusion. The objectives were to elucidate the mechanism of drug release from obtained extrudates and milled strands addicted to the solid-state properties of the solid dispersions and to examine and eliminate stability problems occurring under storage, exposure of mechanical stress, and in vitro dissolution.

Transparent extrudates containing up to 60% drug could be prepared with a temperature setting below the melting point of celecoxib. XRPD and DSC measurements indicated the formation of a glassy solid solution, where the drug is molecularly dispersed in the carrier. The amorphous state of the glassy solid solution could be maintained during the exposure of mechanical stress in a milling process, and was stable under storage for at least 6 months. Solid-state properties and SEM images of extrudates after dissolution indicated a carrier-controlled dissolution, whereby the drug is molecularly dispersed within the concentrated carrier layer. The glassy solid solution showed a 58-fold supersaturation in 0.1 N HCl within the first 10 min, which was followed by a recrystallization process. Recrystallization could be inhibited by an external addition of HPMC.

1. Introduction

Hot-melt extrusion has attracted a considerable interest in describing an efficient production process for pharmaceutical drug delivery systems [1]. With regard to this technique, a wide scope of different dosage forms covering oral, parenteral, and topical applications have been investigated. More specifically, Breitenbach [2] describes the development of melt extrusion in pharmaceutical manufacturing operations and discusses the advantages and drawbacks of the application of melt extrusion technology in the production of solid dispersions. Disadvantages of this technology are often related to high energy input, which can be a strain on thermally sensitive drugs or systems.

Six et al. [3] investigated the influence of the extrusion temperature on the physical state of solid dispersions with itraconazole and Eudragit® E. They performed experiments at two temperature settings, whereby one was adjusted above (heating zones: 50, 79, 170, 175, and 179 °C) and one below (heating zones: 49, 103, 131, 133, and 140 °C) the melting point of itraconazole (168 °C for stable crystalline form). Depending on the drug concentration, they obtained single molecular dispersions or a molecular dispersion in combination with a second phase of pure amorphous itraconazole at 179 °C. Below the melting point of the drug, the second phase consisted of pure crystalline itraconazole.

The efficacy of a drug is mainly defined by the formulation and its solid state. The physical state of the drug in the melt-extruded formulations reaches from simple crystalline embeddings to amorphous or molecularly dissolved stages [4,5]. Therefore, the study of the nature of the solid state is indispensable for the understanding of the mechanism of dissolution enhancement.

The mechanism by which drugs may be released from hot-melt extruded solid dispersions and the processing of the strands to solid dosage forms are issues that are not completely clarified yet. Corrigan and Craig [6,7] highlighted the theories of dissolution with regard to the solid-state structure and dissolution properties of solid dispersions.

Overall, there appears to be two sets of observations that describe the mechanism of drug release from solid dispersions: carrier- or drug-controlled dissolution [7]. In the first instance, the rate of release is controlled by that of the carrier and is independent of the drug properties. In the second instance, mostly observed in conjunction with high drug loads, the dissolution is dominated by the properties of the drug itself [6].

Additional problems of solid dispersions are caused by their thermodynamic instability under storage and especially under

* Corresponding author. Heinrich-Heine-University, Institute of Pharmaceutics and Biopharmaceutics, Universitaetsstrasse 1, Building 26.22, 40225 Duesseldorf, Germany. Tel.: +49 211 8114220.
E-mail address: kleinebudde@uni-duesseldorf.de (P. Kleinebudde).

0939-6411/$ - see front matter © 2008 Elsevier B.V. All rights reserved.
doi:10.1016/j.ejpb.2008.10.002

drug release. One strategy to solve this problem is to increase the solubility of the drug in a polymeric carrier and then to control drug release by incorporation of a second excipient as described by Zhu et al. [8].

The objective of this study was to elucidate the mechanism of dissolution enhancement and to establish a connection between the nature of solid state, the dissolution proceedings and the stability of the system. Therefore, the transformation of the crystalline state of the drug to the amorphous form was examined with regard to the physical characteristics, the dissolution rate and the recrystallization tendency. As there is insufficient knowledge on the processing to oral dosage forms, additionally the influence of mechanical stress on the solid dispersions was investigated.

2. Materials and methods

2.1. Materials

Celecoxib, CEL (Aarti Drugs, Mumbai, India) a selective cyclooxygenase-2 inhibitor, was used as model drug. The BCS Class II drug [9] with a melting point of 162 °C has a pK_a of 9.68 and a low aqueous solubility of about 3 mg/L. CEL was applied in micronized form with a median particle size of 27.8 μm. The cationic basic butylated methacrylate copolymer Eudragit® E PO (aPMMA) with a median particle size of 9.3 μm was kindly donated by Evonik (Darmstadt, Germany). Cetrimide, a mixture mainly consisting of trimethyltetradecylammoniumbromid, was purchased from Fagron GmbH & Co. KG (Barsbuettel, Germany). HPMC (Pharmacoat® 606) was provided by Syntapharm (Muelheim, Germany). Demineralized water was used to prepare the dissolution medium. Hydrochloric acid and potassium bromide were of analytical grade.

2.2. Preparation of melts

For preliminary testing, approximately 2–4 g of the drug or the drug/carrier blend were molten. All blends were prepared with mortar and pestle. The substances were molten at 165 °C in a drying oven under vacuum, cooled at room temperature and milled in an analytic mill (A10, Janke & Kunkel, IKA-Labortechnik, Staufen, Germany).

2.3. Preparation of extrudates and milled strands

Hot-melt extrusion was performed using a co-rotating twin-screw extruder (Leistritz Micro 18, Nuremburg, Germany) with a length-to-diameter ratio of 30. The components were pre-blended in a laboratory scale blender (CML-10, Glatt, Binzen, Germany). The physical mixture was fed with a gravimetric powder feeder (K-Tron, Pitman, NJ, USA). The powder feed rate was set at 0.6 kg/h and the screw speed at 140 rpm. The temperature settings of the barrel segments are shown in Fig. 1.

The molten mass was extruded through a die plate with eight holes having a diameter of 1.0 mm. Hot-melt extrudates were collected from the end of the die and were cooled at room temperature.

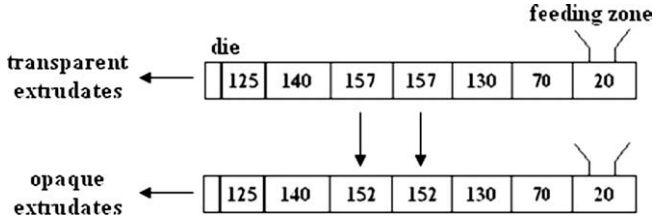

Fig. 1. Temperature profiles [°C] of the extruder barrel for the production of transparent and opaque strands of CEL/aPMMA 1:1 (w/w).

Extrudates were milled at 6000 rpm in a centrifugal mill (Retsch ZM 200, Haan, Germany) with an insert of 1.0 mm. The powder was divided into three fractions (0–125, 125–315, and 315–500 μm) by sieving (AS Control 200, Retsch, Haan, Germany).

2.4. Calculation of three-dimensional solubility parameters

Three-dimensional solubility parameters to polar systems by Hansen were calculated by a computer program (SPWin, version 2.1, Breitkreutz) [10], which contains an advanced parameter set that is based on the group contribution methods of Fedors and Van Krevelen/Hoftyzer [11,12] which were optimized by Breitkreutz.

2.5. Prediction of glass transition temperature

The Gordon–Taylor equation [13] simplified by the application of the Simha–Boyer rule [14] describes the glass transition temperature (T_g) of a binary mixture (Eq. (1)).

$$T_g = \frac{w_1 T_{g_1} + K w_2 T_{g_2}}{w_1 + K w_2}, \quad K \approx \frac{\rho_1 T_{g_1}}{\rho_2 T_{g_2}} \tag{1}$$

Eq. (1): Gordon–Taylor equation simplified by the application of the Simha–Boyer rule; w_i = weight fractions of the components, K = parameter, ρ_i = densities of the amorphous components, subscript 2 = compound with the higher T_g.

The correspondence of experimental data with the Gordon–Taylor equation serves as a criterion of ideality for mixing of the two components [15].

2.6. Differential scanning calorimetry (DSC)

Differential scanning calorimetry was used to determine the glass transition temperature (T_g) of individual components and drug/carrier blends and to examine the solid-state character of the extrudates. Measurements were carried out using a DSC 821e (Mettler-Toledo, Gießen, Germany). Samples of approximately 2–3 mg were sealed in pierced aluminum pans of 40 μl and were measured at a scanning speed of 10 K/min over a temperature range of 293–453 K. The samples were cycled twice to remove the effects of moisture and thermal history. The glass transition temperature was measured in the second cycle as the step transition in the plot of heat flow versus temperature. The solid-state characteristics were surveyed in the first heating cycle by observing the melting enthalpy of the drug. Miscibility of drug and carrier is detected by changes in the melting endotherms of the drug and by the temperature of the glass transition of the blend in comparison to the single T_g of drug and carrier. An empty pan served as reference.

The calibrations of temperature and enthalpy were performed with indium, zinc, and cyclohexane.

2.7. Karl–Fischer titration

The water contents of CEL melts, polymethacrylate melts and their solid dispersions with a drug load of 50% were determined by Karl–Fischer titration (Mettler DL 18, Mettler-Toledo, Giessen, Germany).

2.8. X-ray powder diffraction (XRPD)

The crystallinity of the milled extrudates was measured using a Miniflex apparatus (Rigaku, Muenchen, Germany) with CuKα radiation. Samples were prepared in aluminum frames. For the

preparation, the front of the frames was mounted on a smooth Teflon plate. The samples were filled into the window and were compressed with a slide. This procedure avoided a preferential orientation of the particles.

Diffraction patterns were obtained at a voltage of 45 kV and at a current of 40 mA. Samples were scanned in a 2 theta range from 5° to 40° with a scanning speed of 2 °/min and an intensity of 1000 cps.

2.9. Fourier-transform infrared spectroscopy (FTIR)

FTIR spectra of CEL, polymethacrylate and the solid dispersion were obtained on a Nicolet FTIR 100 spectrophotometer (Thermo Electron Corporation, Waltham, USA). Sample-KBr-blends were compressed into KBr disks in a hydraulic press (Perkin–Elmer, Überlingen, Germany).

2.10. Scanning electron microscopy (SEM)

Samples were coated with gold for 180 s under argon atmosphere using an Agar Manual Sputter Coater (Agar Scientific, Stansted, UK). Coated samples were mounted onto specimen stubs with double-sided carbon tape, and were scanned under high vacuum with a LEO VP 1430 (Carl Zeiss, Jena, Germany).

The morphologies of the milled strands, the extrudates and the extrudates exposed to dissolution were observed at magnifications of 100× and 500×.

2.11. Intrinsic dissolution

The intrinsic dissolution was determined according to Ph.Eur. 5.4. The physical mixture was molten, cooled at room temperature and milled. Three hundred milligrams of the particle fraction 125–315 μm was compacted with a hydraulic press for 30 s with a load of 1 t. Samples with a well-defined surface (diameter 13 mm) were positioned in 900 mL of 0.1 N HCl + 0.15% cetrimide with a rotating speed of 100 rpm. To calculate the intrinsic dissolution rate, the cumulative amount dissolved was plotted against time until 10% related to the saturation solubility were dissolved. Linear regression was performed on data points up to and including the time point beyond which 10% was dissolved. The intrinsic dissolution rate (mg/min) is given by the slope of the regression line. The amount of CEL was detected spectrophotometrically at 250 nm.

2.12. Dissolution study

Drug release from extrudates and milled extrudates was conducted in 900 mL of 0.1 N HCl as dissolution medium for the extrudates and 0.1 N HCl + 0.3% cetrimide for the milled strands using the paddle method (Ph.Eur. 5.3. apparatus 2). The rotational speed of the paddles was set at 50 rpm. A UV wavelength of 250 nm was selected for the spectrophotometrical detection, which is specific for CEL and is free from interference with the polymethacrylate and cetrimide spectra. Measurements were performed in triplicate. Samples for the SEM were released for 2 min in 0.1 N HCl, washed with demineralised water and dried at room temperature.

By the addition of cetrimide to the dissolution medium, the saturation solubility of celecoxib in the dissolution medium is increased. Under sink conditions, i.e. with cetrimide, the concentration of the celecoxib sample in the dissolution medium is below the saturation solubility. Under non-sink conditions, i.e. without cetrimide, the concentration of celecoxib in the dissolution medium is above the saturation solubility, which leads to a supersaturated metastable solution.

HPMC is added to the dissolution medium to evaluate the ability of recrystallization inhibition. This procedure enables an addition to the external phase of a capsule or tablet formulation and keeps the extrusion process as simple as possible with only one excipient.

2.13. Stability testing

Long-term (25 °C, 60% RH, open storage) and accelerated (40 °C, 75% RH, closed storage in aluminum foil) stability testing according to the ICH harmonised tripartite guidelines "Stability testing of new drug substances and products Q1A (R2)" (2003) was performed to determine the physical stability of the solid dispersions under the influence of the environmental factors, temperature and humidity. Samples were stored in a conditioning cabinet (KBF 240, Binder, Tuttlingen, Germany) for storage at accelerated conditions. In this study, stability data for six months are presented as the tests are still ongoing.

3. Results and discussion

3.1. Extrudate characteristics and dissolution behaviour

Transparent extrudates with a drug load of 50% can be produced with the temperature profile described in Fig. 1. Decreasing the temperature in the central part of the extruder barrel leads to opaque strands of CEL and aPMMA, which are the result of insufficient dissolution of the drug in the molten carrier.

Extrudates were characterized regarding their dissolution behaviour in 0.1 N HCl under non-sink conditions employing the paddle method according to Ph.Eur. for 30 min. Crystalline CEL has a saturation solubility of 3 mg/L in this medium. Solubility and dissolution rate of the drug cannot be improved noticeably by physical mixing with aPMMA. The drug release from the opaque extrudate results in a low supersaturation within the first 10 min, whereas the transparent extrudate reaches a 58-fold supersaturation (Fig. 2). Subsequently, both extrudates show similar profiles. As the dissolution of both extrudates ends up with the same dissolved drug amount after 10–15 min, the physical state of the drug in the carrier has a subordinate influence on the second part of the dissolution profile.

Amorphous substances have a higher solubility than the corresponding thermodynamically stable crystalline forms, because their internal bonding forces are weak. Solutions derived from amorphous forms are supersaturated, and crystallization begins as soon as a crystal of the stable form develops. This process is triggered off when the amorphous drug gets into contact with the dissolution medium.

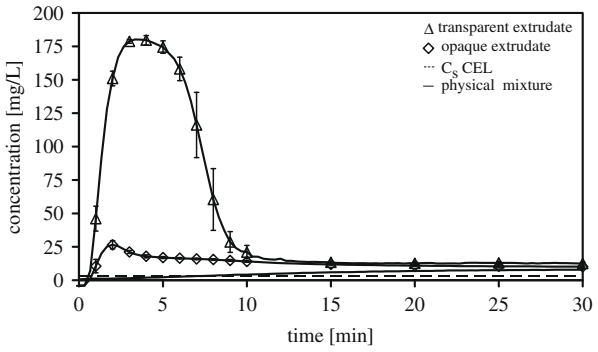

Fig. 2. Drug release of CEL, CEL/aPMMA 1:1 (w/w) physical mixture, CEL/aPMMA 1:1 (w/w) transparent extrudate, and CEL/aPMMA 1:1 (w/w) opaque extrudate; 200 mg drug; 900 mL 0.1 N HCl, non-sink conditions, 37 °C, paddle, 50 rpm, 250 nm; mean ± SD, $n = 3$.

The mechanism underpinning the observed improvements can be described by the formation of a solid dispersion for both strand samples [16].

CEL has a molecular weight of 381 and the aPMMA monomer of 257. Assuming a chemical interaction between the acidic sulfonamide of CEL and the basic dimethylamine of aPMMA, a stoichiometric 1:1 mixture with 60% CEL load would still result in the formation of a glassy solid solution. In order to evaluate the existence of chemical interactions between drug and carrier, FTIR spectra of the pure substances and the melt were examined.

The parts of the FTIR spectra highlighted in Fig. 3 show the stretching vibrations in the area between 3600 and 2600 cm^{-1}. As in the 1:1 (w/w) extrudate, the amount of aPMMA monomer molecules is higher than the amount of CEL molecules, specifically the changes in the CEL signals were compared. The signals of aPMMA are less expressive because a surplus of the carrier is given. The bands at 3339 and 3232 cm^{-1} are seen as doublet, which are attributed to the N–H stretching vibration of the $–SO_2NH_2$ group. In the spectrum of the CEL/aPMMA melt the bands corresponding to N–H stretching of the $–NH_2$ group become diffused and broadened indicating the formation of an amorphous form [17].

The issue of molecular interactions of crystalline and amorphous CEL has been studied in more detail by Gupta et al. [18,19]. They point out that CEL exhibits molecular arrangements in the form of H-bondings for all its electron donors (O of the sulfonyl group, 2-N of the pyrazole ring, and F atom of the trifluoromethyl group). The carbonyl group of the carrier, being a stronger electron donor than the sulfonyl group of the drug, might be favoured in H-bonding resulting in the stability and solubility advantages [20]. The C=O stretching band for both pure aPMMA and the solid dispersion is detected at a frequency of 1729 cm^{-1} (data not shown). Thus, hydrogen bonding between the C=O of the carrier and the NH_2 group of sulfonamide moiety present in CEL, which would be indicated by shifts in frequencies, cannot be proven.

3.2. Solid-state structure

Hansen's three-dimensional solubility parameters of CEL and aPMMA were calculated to predict the miscibility of these components in the molten state [21]. By separate consideration of the sum of intermolecular forces that form cohesive energy, it is possible to elucidate the ability of a molecule to interact with another one via intermolecular forces. Therefore, Hansen defined partial solubility parameters that describe intermolecular dispersion or Van der Waals forces (δ_d), intermolecular polar forces (δ_p), and intermolecular hydrogen bonding (δ_h) [10]. Table 1 shows the values calculated by the computer program. There is a high similarity between the solubility parameters of intermolecular dispersion forces and intermolecular hydrogen bonding. The total solubility parameters indicate a miscibility of both components in the molten state, since their values have a difference of only 5 $MPa^{0.5}$.

The Gordon–Taylor equation is one means of predicting the T_g of a drug/carrier blend in miscible systems based on the T_g, the densities, and the weight fractions of the pure components. Theoretical and experimental T_g of drug/carrier blends were compared to evaluate the influence of the drug content on the T_g of the blend.

Often, drugs have a plasticizing effect on the polymers [22]. They settle between the polymer chains and decrease the interaction between the polymer molecules. The chains become more flexible and the glass transition temperature of the polymer decreases. In the case of celecoxib and aPMMA both a plasticizing and an antiplasticizing effect can be observed (Fig. 4). At a drug content of up to 25%, the drug has a plasticizing effect on the polymer as the T_g of the blend is below the T_g of the pure polymer. At higher drug contents, CEL has an antiplasticizing effect on the polymer. From 60% drug content onward, the T_g reaches the T_g of the pure amorphous drug, which indicates that the properties of the drug dominate. A 1:1 (molar fraction for aPMMA monomer) blend of CEL and aPMMA has a drug content of 60%. At drug loads higher than 60%, CEL is present in a surplus amount, thus, dominating the properties of the melt.

Transparent and opaque extrudates are examined by DSC in order to determine whether the drug is completely molten or dissolved in the carrier or whether crystalline amounts are still detectable. Fig. 5 shows the DSC patterns of the transparent and opaque extrudates. For the transparent extrudate, a single glass transition temperature at 53 °C only is observed, while for the opaque sample a T_g at 53 °C and additionally an endothermic melting peak at the melting point of CEL is detected. The melting point of the pure drug is 25 °C above this peak, which indicates an

Table 1
Three-dimensional solubility parameters (δ_d) of drug and carrier; δ_d = dispersion forces, δ_p = polar forces, δ_h = hydrogen bonding, δ_{tot} = total solubility parameter.

	δ_d, $MPa^{0.5}$	δ_p, $MPa^{0.5}$	δ_h, $MPa^{0.5}$	δ_{tot}, $MPa^{0.5}$
CEL	21.26	7.73	10.88	25.10
Polymethacrylate	17.41	0.20	9.28	19.73

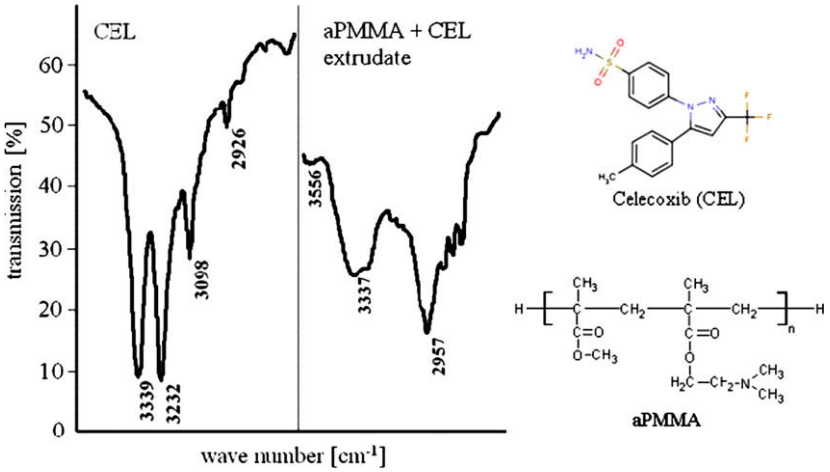

Fig. 3. FTIR spectra of pure CEL and transparent CEL/aPMMA 1:1 (w/w) extrudate.

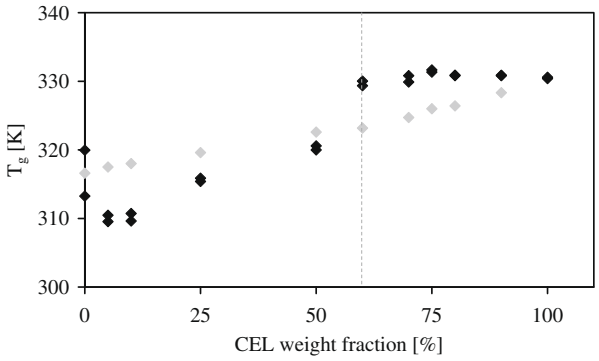

Fig. 4. Influence of CEL drug load on the glass transition temperature of the carrier aPMMA; black symbols = experimental T_g, grey symbols = expected T_g according to Gordon–Taylor (ρ_{CEL} = 1.40 g/cm^3, ρ_{aPMMA} = 1.11 g/cm^3); broken line indicates 1:1 molar fraction; the points at CEL 0% represent the T_g of pure aPMMA.

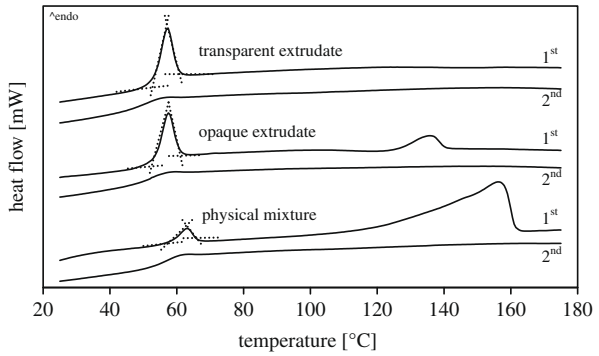

Fig. 5. DSC patterns of transparent and opaque CEL/aPMMA 1:1 (w/w) extrudates and CEL/aPMMA 1:1 (w/w) physical mixture; 1st indicates first heat scan, 2nd second heat scan; heating rate 10 K/min.

interaction of the drug with the molten carrier. These results point to an amorphous one-phase system for the transparent and an amorphous and crystalline two-phase system for the opaque extrudates.

During the extrusion process, the formation of a glassy solid solution is additionally supported by mixing and shearing of the molten mass. The DSC analysis of the transparent extrudates indicates again the formation of a glassy solid solution (Fig. 5) as a single T_g during the first heat scan – equivalent to the second heat scan in the DSC – only can be detected [23].

These results confirm the assumption that a homogeneous one-phase system is built wherein the particle size of the drug is reduced to a minimum state, i.e. its molecular size.

3.3. Drug load

Poorly water-soluble drugs often have to be administered in a high dose. Therefore, only a small amount of excipients can be added to the formulation in order to preclude difficulties relating to patient compliance. Thus, it is important to be able to produce solid dispersions containing as much of the active substance as possible. The maximum load with CEL for aPMMA was tested by intrinsic dissolution studies. Compacts with drug loads of 5, 10, 25, 50, 62.5, 75, and 100% (w/w) were dissolved in 0.1 N HCl + 0.15% cetrimide, and the dissolution rate was deduced from the slope of the particular dissolution profiles.

As shown in Fig. 6, the dissolution rate is controlled by the drug/carrier ratio of the formulation. The dissolution rate increases by increasing the drug amount in the blend up to a drug load of 50% and decreases markedly from amounts higher than 50%. This

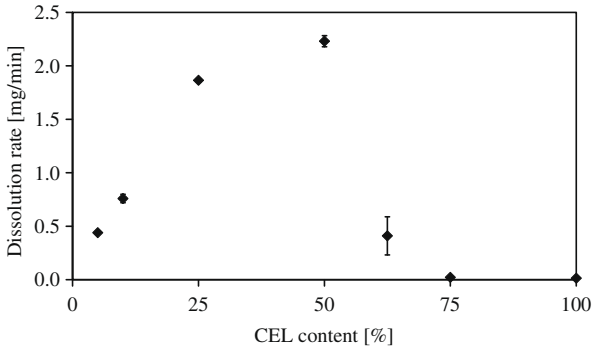

Fig. 6. Preliminary testing of the influence of the drug content on the dissolution rate of the solid dispersion; mean ± SD; n = 3.

examination shows that the maximum drug load for the CEL/aPMMA blend lies between 50 and 62.5%. This observation leads to the assumption that the improvement of drug release is based on a chemical interaction between drug and carrier. As a stoichiometric 1:1 proportion of CEL and the aPMMA monomer is realized at a drug load of 60%, the results indicate that above this drug load a surplus of crystalline drug is present in the formulation which sets off recrystallization and, therefore, dominates the dissolution properties of the solid dispersion.

As additional shear and mixing forces in the extruder might enable a higher drug load, this assumption was verified in an extrusion process [24]. Therefore, a blend with a drug content of 62.5% drug was extruded, but no transparent strands could be produced. Thus, the maximum drug load for the formation of glassy solid solutions could be predicted by these preliminary experiments.

3.4. Mechanism of dissolution enhancement

Knowledge of the mechanism of drug release from solid dispersions is essential for understanding the enhancement in the dissolution rate of a poorly soluble drug. Two mechanisms of drug release from solid dispersions are known from the literature [6,7]. Carrier-controlled dissolution occurs in case the drug release is dependent on the properties of the carrier. Drug-controlled dissolution predominates in case the drug release is dependent on the properties of the drug. In order to reveal the mechanism of drug release from CEL/aPMMA solid dispersions, the glassy solid solution (transparent) and the crystalline glass suspension (opaque) were dissolved in 0.1 N HCl for 2 min and then examined in more detail. The surface morphology of the strands and the release mechanism can be visualized by SEM studies [25]. Fig. 7 shows the images of the strands before and after dissolution. Two processes take place. The first one is recrystallization of the opaque strands when getting into contact with the dissolution medium. The second one is a dissolving process, which becomes obvious when comparing the thickness of the strands before and after dissolution. After 2 min dissolution, the thickness of the transparent strand has decreased to a higher extent than the thickness of the opaque strand, which corresponds with the dissolution profile in Fig. 2.

Thus, two different mechanisms can be defined. The crystalline glass suspension follows a drug-controlled dissolution, because the rate-determining step is the dissolving of the poorly water-soluble drug. Consequently, the dissolution is not associated with the polymer but is, instead, dominated by the poor solubility properties of the drug. The glassy solid solution follows a carrier-controlled dissolution, because the particles are molecularly dispersed in the carrier and are, therefore, dissolved into the polymer-rich diffusion layer together with the carrier.

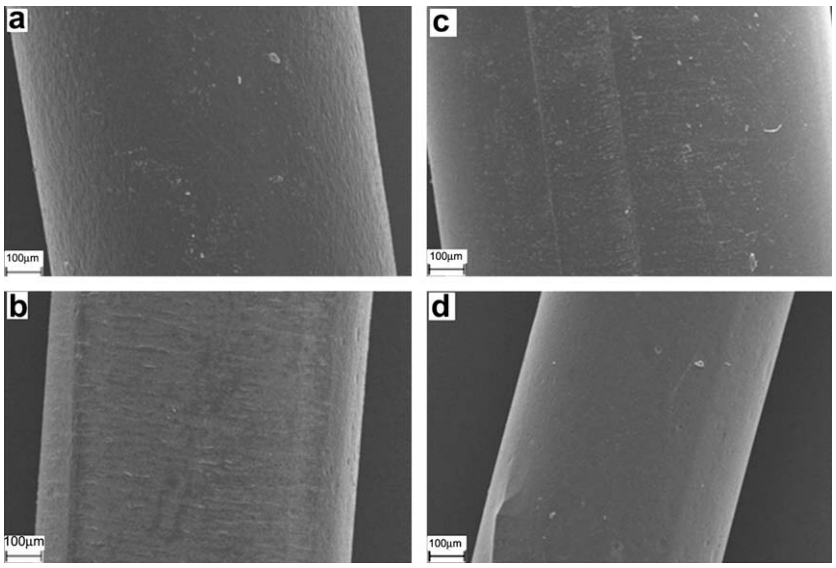

Fig. 7. SEM images of opaque (a and b) and transparent (c and d) aPMMA/CEL 1:1 (w/w) extrudates before (a and c) and after (b and d) 2 min dissolution; high voltage 20 kV.

3.5. Stability on storage

Glassy solid solutions are thermodynamically metastable systems that favour the conversion to the crystalline form under storage [26]. Evolving crystalline structures can be detected by XRPD analysis as arising peaks from the halo pattern.

In order to test the stability of the glassy solid solution under storage, the extrudates were characterized by XRPD directly after preparation and after storage at room temperature located on top of silica gel. Fig. 8 shows the XRPD patterns of pure CEL, the physical mixture 1:1 (w/w), and the milled extrudates. Since the extrudate in its form of a glassy solid solution does not consist of any crystalline structures, the pattern shows a halo without any peaks. After storage for six months, no recrystallization can be found in the pattern of the milled extrudates indicating a good physical stability.

Regarding amorphous systems, two conflicting phenomena are associated with the crystallization process. While the rate of nucleation may be expected to increase with lowering temperature, the molecular mobility decreases, thereby slowing the molecular diffusion and reducing the rate of crystallization. Therefore, the maximum rate of crystallization will take place between T_m and T_g [26].

In studies by Hancock and Zografi [27], a glass transition of the glassy solid solution system of approximately 50 °C above the storage temperature is demanded to preclude recrystallization of the amorphous system. Even for CEL formulations, the antiplasticizing effect on polymers with a high T_g is described [28]. In this case, the T_g is much lower at 52 °C, but does not present a disadvantage for the storage stability.

The inclusion of water has a negative influence on the stability of glassy solid solutions. This impact results from the water uptake of the respective polymer. Especially polymers with hydrophilic functional groups tend to take up a high amount of water. Additionally, water has a negative effect on the stability of amorphous substances. Amorphous forms represent metastable systems, which are more stable if the glass transition temperature is high. As water can decrease the T_g, the amorphous system tends to recrystallize earlier.

Therefore, the water uptake of the drug melt, of the carrier melt, and of the molten 1:1 blend of both substances was examined. All samples were stored under two different conditions: at 25 °C over silica gel and at 40 °C, 75% relative humidity for 6 months. Fig. 9 shows that the water uptake of all samples is below 2% and, therefore, quite low. The pure carrier melt and the molten blend take up small amounts of water, when stored at 75% relative humidity. The pure drug melt is unbiased, as the amount of water is the same under both storage conditions. Amorphous CEL recrystallizes within the first few days after production. Therefore, the data represent rather the water uptake of the crystalline drug and not of the amorphous form.

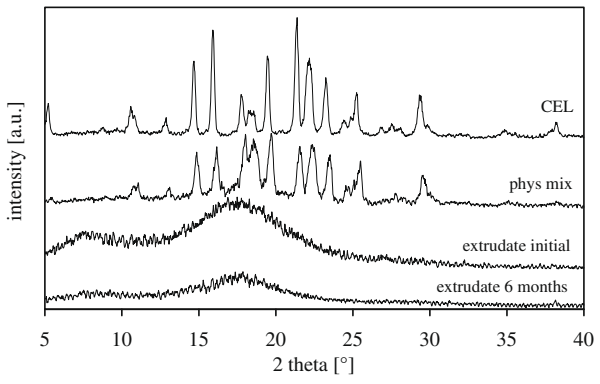

Fig. 8. XRPD patterns of CEL, CEL/aPMMA 1:1 (w/w) physical mixture, and CEL/aPMMA 1:1 (w/w) extrudates after extrusion (initial) and after storage at 25 °C, 60% relative humidity (6 months); extrudates were milled for sample preparation.

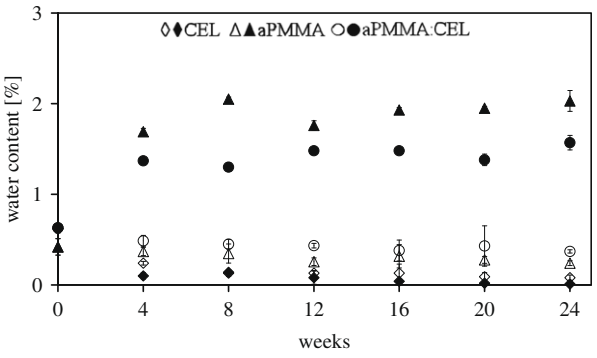

Fig. 9. Water uptake of CEL melt, aPMMA melt, and molten blend of CEL and aPMMA 1:1 (w/w) examined by Karl–Fischer titration; open symbols represent storage at 25 °C over silica gel, closed symbols represent storage at 40 °C, 75% relative humidity; mean ± SD; $n = 3$.

In this case, the properties of the blend are more strongly influenced by the properties of the carrier as their behaviour towards water uptake is more alike than compared to the pure drug melt. Overall, the effect of water seems to be negligible for systems with aPMMA.

3.6. Stability on mechanical stress and influence of the particle size on dissolution

For the formulation of solid dosage forms, the extrudates must be processed further. This can be realized by cutting or milling the strands into granules, pellets or fine powder. These processing steps are accompanied by a mechanical energy input, which might be harmful to the glassy solid solution formulations. As glassy solid solutions represent metastable systems, they often tend to recrystallize during milling. In order to evaluate the susceptibility to precipitation under mechanical energy input, the extrudates were milled and tested for solid-state transformations by XRPD analysis.

Fig. 10 shows the XRPD patterns of pure crystalline CEL, the extrudates before milling, and the milled extrudates. The halo of the milled extrudates exhibits no peaks from the crystalline CEL, which implies that the powder still remains in its amorphous form. Hence, grinding has no influence on the stability of the glassy solid solution.

The dissolution rate of the extrudate is increased in comparison to that of crystalline drug substance and physical blends of the drug and the carrier (Fig. 2). Additionally, the dissolution rate can be directed by the particle size. Fig. 11 shows that small particles result in faster dissolution profiles due to larger surface areas. This observation, for instance, can be used for the production of pellets or the choice of particle size in tablet formulations.

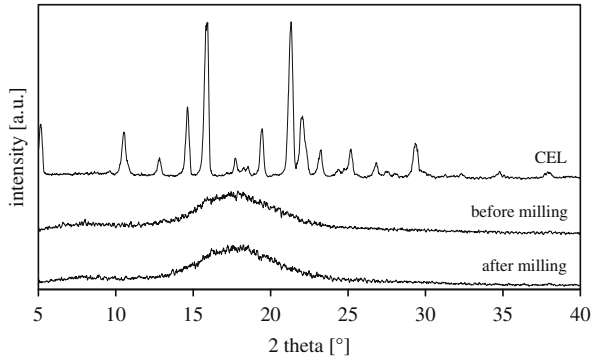

Fig. 10. XRPD patterns of pure CEL, CEL/aPMMA 1:1 (w/w) extrudates (before milling), and CEL/aPMMA 1:1 (w/w) extrudates after milling.

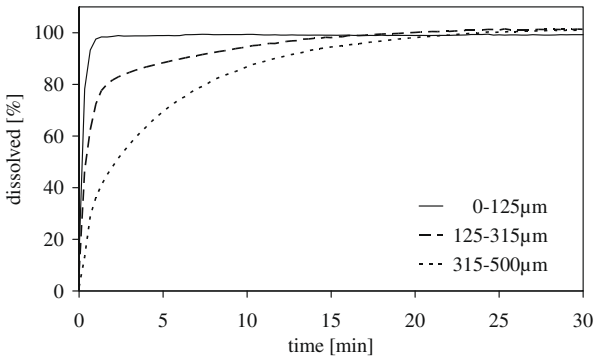

Fig. 11. Dissolution profiles of milled extrudates; 200 mg drug; 900 mL 0.1 N HCl + 0.3% cetrimide, sink conditions, 37 °C, paddle, 50 rpm, 250 nm; mean ± SD, $n = 3$.

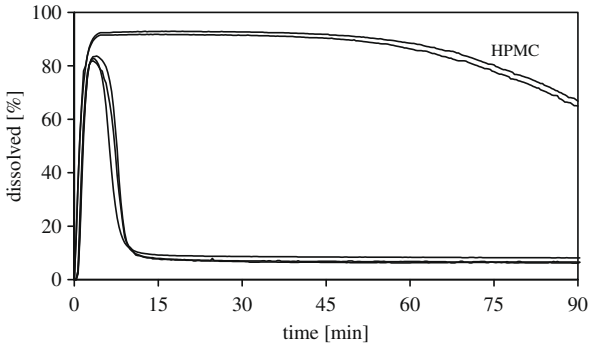

Fig. 12. Dissolution profiles of glassy solid solutions of CEL/aPMMA 1:1 (w/w); 200 mg drug; 900 mL 0.1 N HCl, 0.1 N HCl + 40 mg HPMC; non-sink conditions, 37 °C, paddle, 50 rpm, 250 nm.

3.7. Recrystallization inhibition

Solid dispersions form thermodynamically metastable supersaturated solutions in dissolution testing. Fig. 12 shows the dissolution profiles of the glassy solid solution in 0.1 N HCl and in 0.1 N HCl with an addition of 40 mg HPMC. In this case, the addition of the hydrophilic polymer has two advantages: The supersaturation within the first 10 min reaches a maximum as the drug is released completely in the dissolution medium. Furthermore, the recrystallization process can be delayed for at least 60 min, which represents a promising solution with regard to improved bioavailability.

4. Conclusion

This study has elucidated the mechanisms by which drug is released from solid dispersions. Depending on the solid-state properties, the glassy solid solutions follow a carrier-controlled mechanism, crystalline glass suspensions follow a drug-controlled mechanism. Whether a glassy solid solution or a crystalline glass suspension is produced in the hot-melt extrusion process, this is mainly dependent on the temperature settings of the barrel segments. If the system is undergoing carrier-controlled dissolution, the initial particle size and the physical form of the drug are of minimal importance. Both systems lead to supersaturated solutions, whereas the glassy solid solution reaches a higher initial supersaturation. The glassy solid solutions are stable under storage and mechanical stress and present, therefore, promising possibilities in the processing to solid dosage forms. Since these systems follow a carrier-controlled dissolution ageing effects should be due to the changes in the properties of the carrier. Recrystallization problems during dissolution can be overcome by an external addition of recrystallization inhibitors to the formulation. The external addition helps to prevent interactions between additional excipients during the melting process. Overall, the elucidation of the dissolution process of solid dispersion formulations is a helpful objective to facilitate the development of the associated dosage forms.

References

[1] J. Breitenbach, Feste Lösungen durch Schmelzextrusion – ein integriertes Herstellkonzept, Pharmazie in Unserer Zeit 29 (2000) 46–49.
[2] J. Breitenbach, Melt extrusion: from process to drug delivery technology, European Journal of Pharmaceutics and Biopharmaceutics 54 (2002) 107–117.
[3] K. Six, C. Leuner, J. Dressman, G. Verreck, J. Peeters, N. Blaton, P. Augustijns, R. Kinget, G. Van den Mooter, Thermal properties of hot-stage extrudates of itraconazole and Eudragit E100 – phase separation and polymorphism, Journal of Thermal Analysis and Calorimetry 68 (2002) 591–601.
[4] T. Matsumoto, G. Zografi, Physical properties of solid molecular dispersions of indomethacin with poly(vinylpyrrolidone) and poly(vinylpyrrolidone-co-vinylacetate) in relation to indomethacin crystallization, Pharmaceutical Research 16 (1999) 1722–1728.

[5] A. Forster, J. Hempenstall, T. Rades, Characterization of glass solutions of poorly water-soluble drugs produced by melt extrusion with hydrophilic amorphous polymers, Journal of Pharmacy and Pharmacology 53 (2001) 303–315.
[6] O.I. Corrigan, Mechanisms of dissolution of fast release solid dispersions, Drug Development and Industrial Pharmacy 11 (1985) 697–724.
[7] D.Q.M. Craig, The mechanisms of drug release from solid dispersions in water-soluble polymers, International Journal of Pharmaceutics 231 (2002) 131–144.
[8] Y.C. Zhu, N.H. Shah, A.W. Malick, M.H. Infeld, J.W. McGinity, Controlled release of a poorly water-soluble drug from hot-melt extrudates containing acrylic polymers, Drug Development and Industrial Pharmacy 32 (2006) 569–583.
[9] M. Yazdanian, K. Briggs, C. Jankovsky, A. Hawi, The "high solubility" definition of the current FDA guidance on biopharmaceutical classification system may be too strict for acidic drugs, Pharmaceutical Research 21 (2004) 293–299.
[10] J. Breitkreutz, Prediction of intestinal drug absorption properties by three-dimensional solubility parameters, Pharmaceutical Research 15 (1998) 1370–1375.
[11] R.F. Fedors, Method for estimating both solubility parameters and molar volumes of liquids, Polymer Engineering and Science 14 (1974) 147–154.
[12] D.W. Van Krevelen, P.J. Hoftyzer, Properties of Polymers, Cohesive Properties and Solubility, Elsevier, Amsterdam, 1997.
[13] M. Gordon, J.S. Taylor, Ideal copolymers and the second-order transitions of synthetic rubbers. I. Non-crystalline copolymers, Journal of Applied Chemistry 2 (1952) 493–500.
[14] R. Simha, R.F. Boyer, On a general relation involving the glass temperatures and coefficient of expansion of polymers, Journal of Chemical Physics 37 (1962) 1003–1017.
[15] A. Forster, J. Hempenstall, T. Rades, Comparison of the Gordon–Taylor and Couchman–Karasz equations for prediction of the glass transition temperature of glass solutions of drug and polyvinylpyrrolidone prepared by melt extrusion, Pharmazie 58 (2003) 838–839.
[16] C. Leuner, J. Dressman, Improving drug solubility for oral delivery using solid dispersions, European Journal of Pharmaceutics and Biopharmaceutics 50 (2000) 47–60.
[17] G. Chawla, P. Gupta, R. Thilagavathi, A.K. Chakraborti, A.K. Bansal, Characterization of solid-state forms of celecoxib, European Journal of Pharmaceutical Sciences 20 (2003) 305–317.
[18] P. Gupta, R. Thilagavathi, A.K. Chakraborti, A.K. Bansal, Differential molecular interactions between the crystalline and the amorphous phases of celecoxib, Journal of Pharmacy and Pharmacology 57 (2005) 1271–1278.
[19] P. Gupta, A.K. Bansal, Molecular interactions in celecoxib-PVP-meglumine amorphous system, Journal of Pharmacy and Pharmacology 57 (2005) 303–310.
[20] V.K. Kakumanu, A.K. Bansal, Enthalpy relaxation studies of celecoxib amorphous mixtures, Pharmaceutical Research 19 (2002) 1873–1878.
[21] A. Forster, J. Hempenstall, I. Tucker, T. Rades, Selection of excipients for melt extrusion with two poorly water-soluble drugs by solubility parameter calculation and thermal analysis, International Journal of Pharmaceutics 226 (2001) 147–161.
[22] M.A. Repka, T.G. Gerding, S.L. Repka, J.W. McGinity, Influence of plasticizers and drugs on the physical–mechanical properties of hydroxypropylcellulose films prepared by hot melt extrusion, Drug Development and Industrial Pharmacy 25 (1999) 625–633.
[23] J. Breitenbach, G. Berndl, J. Neumann, J. Rosenberg, D. Simon, J. Zeidler, Solid dispersions by an integrated melt extrusion system, Proceedings: International Symposium on Controlled Release of Bioactive Materials 25 (1998) 804–805.
[24] A. Forster, J. Hempenstall, I. Tucker, T. Rades, The potential of small-scale fusion experiments and the Gordon–Taylor equation to predict the suitability of drug/polymer blends for melt extrusion, Drug Development and Industrial Pharmacy 27 (2001) 549–560.
[25] M.M. Crowley, B. Schroeder, A. Fredersdorf, S. Obara, M. Talarico, S. Kucera, J.W. McGinity, Physicochemical properties and mechanism of drug release from ethyl cellulose matrix tablets prepared by direct compression and hot-melt extrusion 1, International Journal of Pharmaceutics 269 (2004) 509–522.
[26] D.Q. Craig, P.G. Royall, V.L. Kett, M.L. Hopton, The relevance of the amorphous state to pharmaceutical dosage forms: glassy drugs and freeze dried systems, International Journal of Pharmaceuticals 179 (1999) 179–207.
[27] B.C. Hancock, G. Zografi, Characteristics and significance of the amorphous state in pharmaceutical systems, Journal of Pharmaceutical Sciences 86 (1997) 1–12.
[28] P. Gupta, V.K. Kakumanu, A.K. Bansal, Stability and solubility of celecoxib-PVP amorphous dispersions: a molecular perspective, Pharmaceutical Research 21 (2004) 1762–1769.